Communications

Obstacle Avoidance with Ultrasonic Sensors

JOHANN BORENSTEIN AND YORAM KOREN

Abstract—**A mobile robot system, capable of performing various tasks for the physically disabled, has been developed. To avoid collision with unexpected obstacles, the mobile robot uses ultrasonic range finders for detection and mapping. The obstacle avoidance strategy used for this robot is described. Since this strategy depends heavily on the performance of the ultrasonic range finders, these sensors and the effect of their limitations on the obstacle avoidance algorithm are discussed in detail.**

I. Introduction

This communication describes some features of a mobile nursing robot system, which is produced as an aid for bedridden who acquire constant assistance for the most elementary needs. Such a device, it is hoped, will return a measure of independence to many bedridden persons as well as reducing the number of those in need of hospitalization and constant attendance [22], [23]. The workspace of the nursing robot would be usually confined to one room, either in a hospital or in the user's home. This limitation is important since the constant presence of the disabled person as a supervisor for the robot's activities greatly facilitates the design of our system and makes it more economic compared with other similar mobile robots.

Our system is composed of three major subsystems: a mobile carriage, a robot mounted on it, and a computerized post next to the disabled person's bed. To interact intelligently with its environment, the robot utilizes the following sensors:

1) two ultrasonic range finders mounted on the vehicle to detect obstacles and provide information to detour the obstacle;
2) microswitches attached to the vehicle bumpers to detect collisions with obstacles that were not found out by the range finders;
3) incremental encoders attached to the wheels to monitor the incremental position of the vehicle;
4) light sources attached to the walls and a rotating light-detecting sensor located on the vehicle to update the absolute position of the vehicle in the room;
5) force sensors integrated into the robot's gripper to ensure proper handling of various objects;
6) a video camera attached to the arm to permit the detection and acquisition of objects;
7) a speech recognition unit to translate verbal instructions into computer commands.

The prototype of the mobile robot is shown in Fig. 1. It comprises the carriage which houses the computers and the electronic hardware and a commercially available five-degrees-of-freedom (DOF) manipulator. The two ultrasonic transceivers and the light-detecting sensor are attached to joint 1 of the manipulator such that they can rotate about the vertical axis. Fig. 1 also shows the multipurpose gripper with its integrated three-DOF force sensor as well as the floor-level bumper with the microswitches.

Manuscript received June 3, 1986; revised April 22, 1987.

J. Borenstein and Y. Koren are with the Department of Mechanical Engineering and Applied Mathematics, The University of Michigan, 2250 G. G. Brown, Ann Arbor, MI 48109-2125.

IEEE Log Number 8718060.

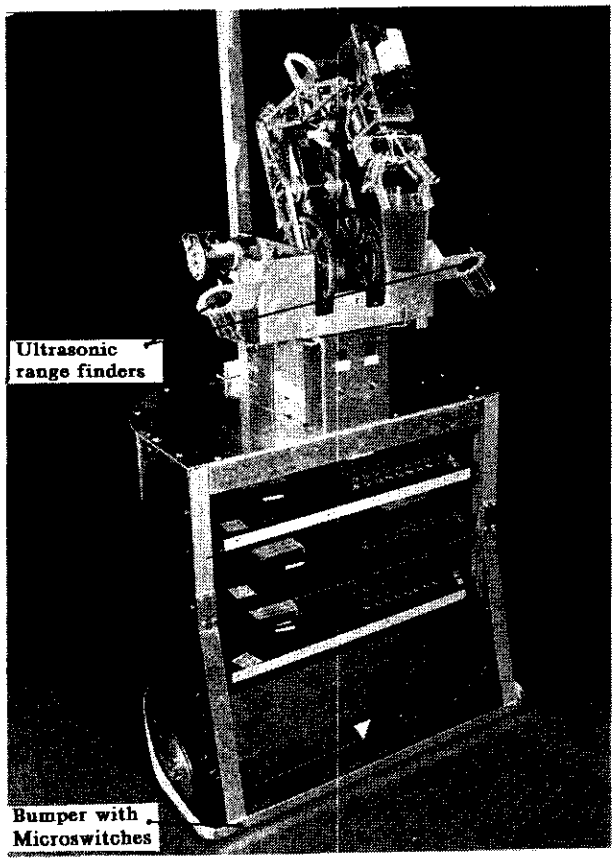

Fig. 1. Technion's nursing robot.

To move from one location A to another location B, the carriage operates according to the following strategy. At first, the carriage rotates about its center until the robot faces exactly into the direction of B (pure rotation). Then the robot moves straight forward until it reaches point B (pure translation), followed by another pure rotation about its center until the carriage has the required final orientation [4].

Any motion between two given locations is performed in this sequence. The peculiarity of this approach is that it actually uses only two distinct kinds of motion, either a motion in a straight line, where both wheels run at the same angular speed in the same direction, or a rotation about the carriage's center, where both wheels run at the same angular speed but in opposite directions. This strategy offers numerous advantages: it is relatively simple yet provides an effective control system; it avoids slippage of the wheels; the carriage path is always predictable; and the carriage always travels through the shortest possible distance (straight line or rotation "on the spot") [2].

II. Limitations of Ultrasonic Range Finders

Ultrasonic range measurements suffer from some fundamental drawbacks which limit the usefulness of these devices in mapping or in any other task requiring high accuracy in a domestic environment. These drawbacks are not related to the product of a specific

0882-4967/88/0400-0213$01.00 © 1988 IEEE

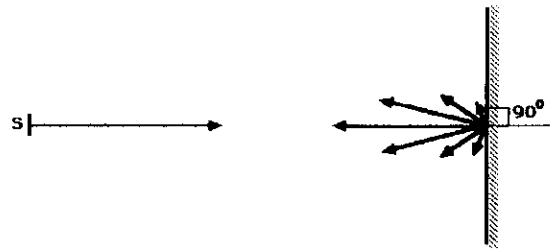

Fig. 2. Reflections of sound waves from smooth surface perpendicular to acoustic axis.

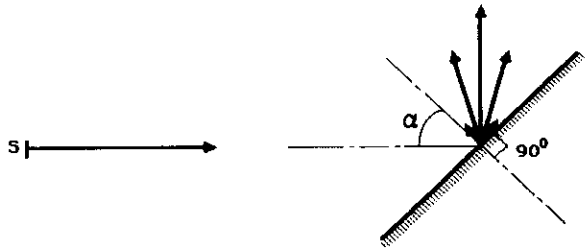

Fig. 3. Reflected sound waves are not received by transducer when angle α is large.

manufacturer, but are inherent to the principle of ultrasonic range finders and their commonly used wavelengths.

Even though ultrasonic ranging devices play a substantial role in many robotics applications [9], [10], [13], [27], [31], only a few researchers seem to pay attention to (or care to mention) their limitations [12], [16]–[18], [26]. In our experiments, one well-established device [5], [7], [8], [14], [15], [24], [30], the Polaroid ultrasonic ranging kit, was used and extensively tested. This unit performed up to our expectations, but, of course, is also subjected to the limitations which are described next.

1) Fig. 2 shows (schematically) one part of the wavefront, emitted by the ultrasonic transceiver S toward a parallel surface of an obstacle (see [26], [28] for more detailed discussion on radiation characteristics of the ultrasonic transducer). Most of the sound energy is reflected perpendicular to the surface and will be detected by S, while only a small percentage of the energy is scattered in other directions. However, if the surface of the obstacle is tilted relative to the acoustic axis of S (as in Fig. 3), then only an undetectably small amount of energy will be reflected toward S. For a mobile robot application this means that the obstacle has not been detected.

Obviously, the amount of reflected sound energy depends strongly on the surface structure of the obstacle. To obtain a highly diffusive reflection from an obstacle, the size of the irregularities on the reflecting surface should be comparable to the wavelength of the incident soundwaves [20]. For the Polaroid ranging unit,

$$\lambda = \frac{v}{f} = \frac{340 \text{ m/s}}{50000 \text{ Hz}} = 6.8 \text{ mm}$$

where

λ	wavelength,
$v = 340$ m/s	velocity of sound waves in air at room temperature;
$f = 50$ kHz	frequency of the sound waves.

Unfortunately, the domestic environment comprises mostly much smoother surfaces, such as walls, polished wood, plastics, etc. Increasing the frequency (thereby decreasing the wavelength) of the sound waves is limited by the undesirable side effect of a higher energy dissipation. The maximum angle of tilt (α in Fig. 3) for a reliable detection of a "smooth" surface has been said to be about 25° [12]. We have found that this angle may be increased to 40–45° by operating with higher gain of the receiver circuit, even though this

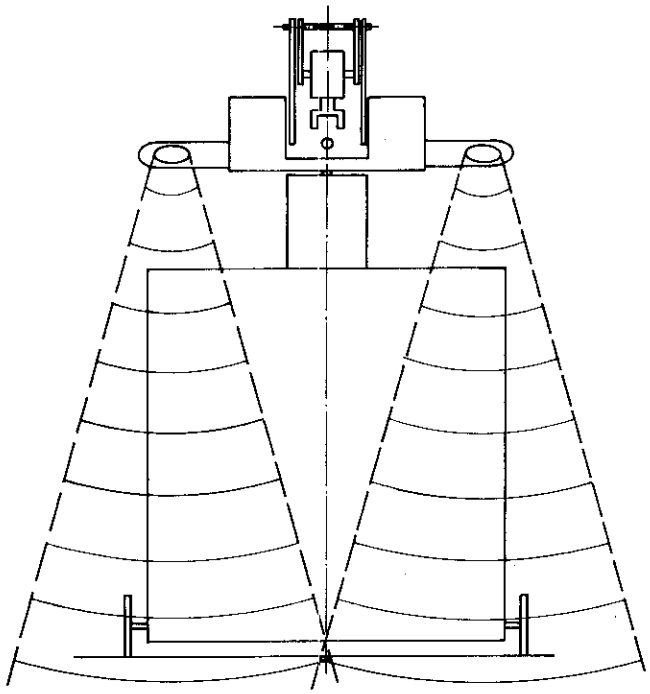

Fig. 4. Scan field for two transducers mounted on "waist"-joint of robot.

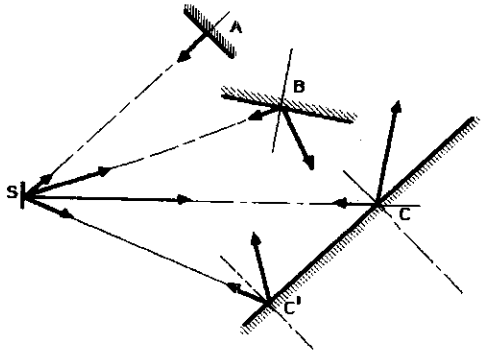

Fig. 5. Directional uncertainty for various obstacles due to wide-angle emission cone.

causes a decrease in directionality of the measurement and occasional misreadings of the measured distances. However, the directionality problem is partly accounted for in our obstacle avoidance algorithm (which will be described later) whereas the misreadings are easily identified since they always read the shortest measurable distance, 27 cm, instead of the actual distance to the object. These misreadings may be discarded simply by discarding any range reading of less than 30 cm. (A lower limit distance reading is provided to allow the transducer's membrane vibrations—after emission of a sound burst—to decay before the same membrane is used to detect reflected sound waves. Technically, the limit is implemented as a minimum time interval within which the receiver circuit is disabled. If the receiver gain is increased too much, even almost completely decayed vibrations will be detected at the end of the minimum time interval and interpreted as an echo. A lower limit on the measurable distance must always exist when a transceiver, rather than separate transmitter and separate receiver, is used.)

2) Another problem arises when the direction to a certain obstacle has to be found precisely. The emission cone of the sound waves is depicted in Fig. 4. The cone has an opening angle of about 20–30°, with increasing energy content towards the acoustic axis. Fig. 5 shows two problems related to this fact. Obstacle A is at the edge of

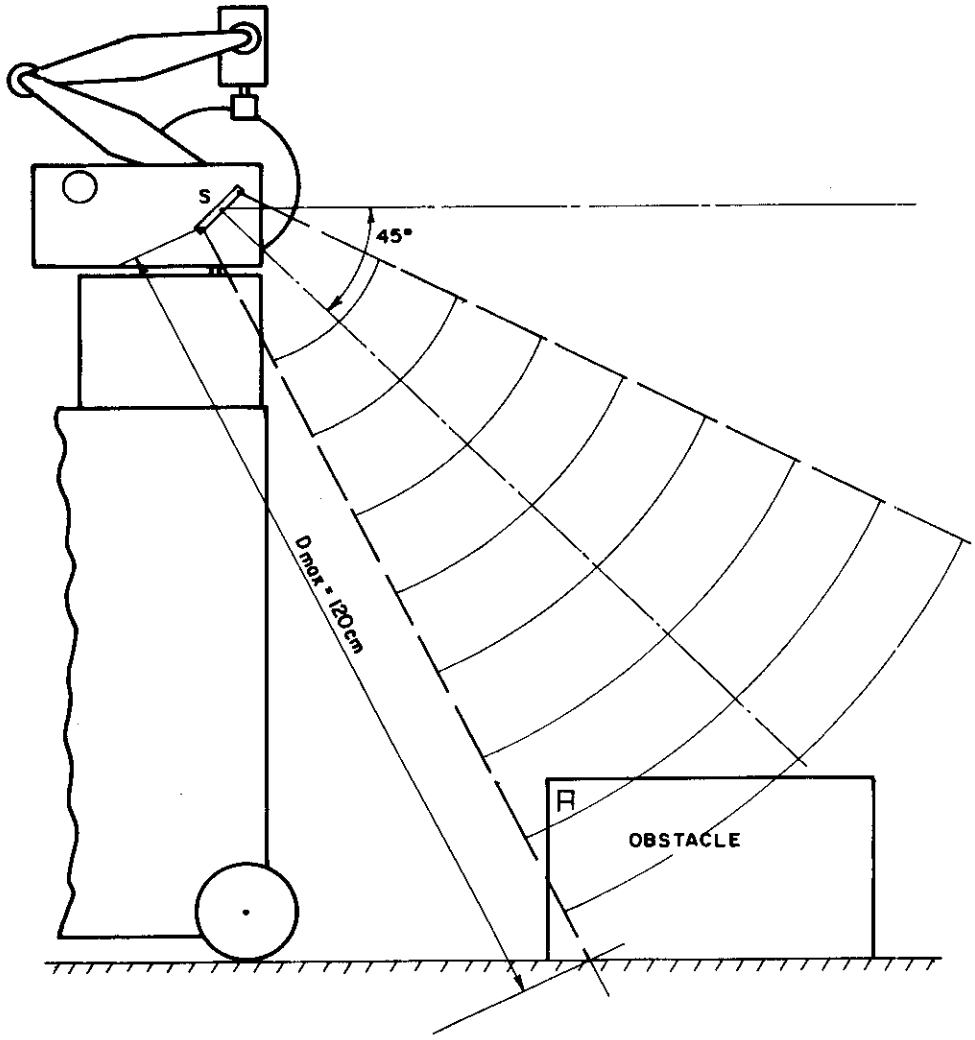

Fig. 6. Transducers pointing to detect obstacles on floor add uncertainty regarding actual distance to obstacle.

the acoustic cone and therefore receives only a small amount of energy from S, whereas its orientation is perpendicular to the incident sound waves, resulting in optimal reflection. Obstacle B, on the other hand, receives more energy from S, being closer to the acoustic axis, but the reflection is poor because of the unfavorable orientation. Therefore, it is not quite clear which—if any at all—of the obstacles is detected. A similar problem arises at C and C'. Here C is on the acoustic axis but has a less favorable orientation then C'. In this case, neither the direction nor the distance to the obstacle can be determined accurately.

Clearly, the latter problems can be minimized by improving the directionality of the transducer (i.e., narrowing the emission cone). This may be achieved by adding special devices such as acoustic lenses [26], [29], [30], or by utilizing transceivers especially designed for high directionality. However, if a wide "field of view" was desired, as is the case with a mobile robot that has to continuously scan the way in front of it, a large number of "narrow-beam" transceivers (each one pointing into a different direction) would be required. For this purpose, some designs are known that use 7 [11], 14 [1], and even 24 [27] or 36 [21] ultrasonic sensors.

In our mobile robot there are only two (rather "wide-angle") transceivers attached to both sides of the waist" joint of the manipulator, as shown in Fig. 4. The transducers are mounted at an angle of 45° with the horizon (Fig. 6), which is required to detect obstacles on the floor. This even increases the uncertainty in measurements of distance and direction of obstacles as shown in Fig. 6. Upon detecting an edge A, the robot measures the distance SA which is obviously greater than the actual distance between the robot and the obstacle. Experiments with randomly chosen domestic objects (e.g., chair, wall, briefcase, etc.) yielded inaccuracies in the location of an object's vertical edges of up to 40 cm.

III. The Ultrasonic Sensor in the Nursing Robot

The mobile nursing robot attempts to reach any given goal inside a room without the disabled person's interference. For this purpose, a "map" of the stationary obstacles (e.g., walls, closets, beds, etc.) is fed into the robot's database during an initial setup phase, when the robot is introduced to a new environment. However, more obstacles (e.g., chairs, tables, etc.) may unexpectedly obstruct the robot's path and must therefore be detected by sensors. In the nursing robot, bumpers with microswitches as well as the two ultrasonic range finders serve this purpose. The latter are used in two distinct modes of operation: scanning mode and measuring mode.

A. Scanning Mode

Whenever the robot moves forward, the scanning mode operates. In this mode, range readings are alternately sampled from both sensors approximately every 40 ms (this corresponds to about 2.2 cm of the robot's straight-line travel at maximum speed). An "obstacle alarm" is issued when the following test results in a "true":

$$\text{IF } R_i(j) < TD \text{ AND } R_i(j) \leq R_i(j-1) \text{ THEN ALARM}$$

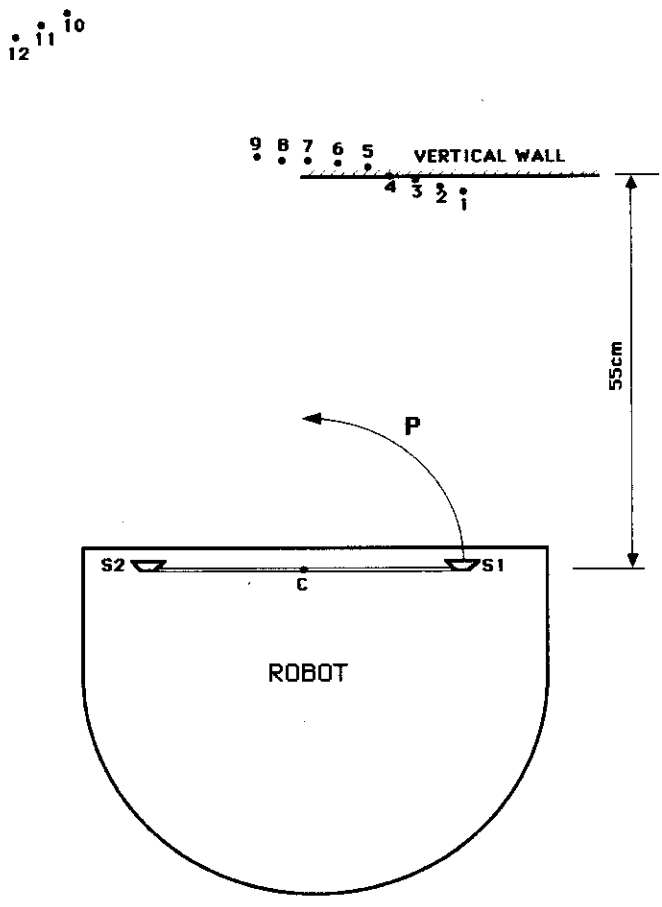

Fig. 7. Typical scan of vertical obstacle.

where

TD	threshold,
$R_i(j)$	range reading of transceiver i,
$R_i(j-1)$	previous range reading of transceiver i.

The value for TD has been determined experimentally as 100 cm, which is 20 cm less than the maximal measurable distance (D_{max} in Fig. 6). The logical meaning of a "true" result for the test is that some obstacle is obstructing the sensor's "view" to the floor *and* that the robot is getting closer to this obstacle. This algorithm has proven very effective in eliminating erroneous readings that may occur for various reasons.

B. Measuring Mode

After the robot has stopped in response to an "obstacle alarm," the ultrasonic sensors are used in the measuring mode. In this mode the robot rotates its manipulator with the ultrasonic transducers attached to it 70° to the left (left scan), back to 0°, and then 70° to the right (right scan) and samples range readings every 2°. A close-to-far transition between subsequent range readings, passing the THRESHOLD level of 100 cm indicates the presence of an edge. Since there could be several closely placed obstacles, the last detected edge is considered the only valid one, thereby lumping together all closely placed obstacles. This is legitimate since the robot could not pass between these obstacles anyway. If no edge is detected when scanning to the left or to the right (this case may occur when the robot is facing a wall), then an edge is assumed at the extreme left or right, accordingly.

Fig. 7 shows the experimental result of a left scan, where the robot is partially facing a vertical wall (plywood). As the transducer $S1$ is swiveled horizontally about the centerpoint C (on path p), range readings are taken every (only in this example) 3°. After recalculation of measured distances (to account for the 45° tilt of the transducer, as well as for variation in actual distance to the wall, because of path p), points 1–12 are found. Points 1–9 represent reflections from the wall, whereas points 10–12 result from reflections from the floor at the maximal distance D = 120 cm. The close-to-far transition occurs after point 9, which is therefore identified as the obstacle's "left" edge. Only this point is retained in memory. A subsequent right scan (results are not plotted in Fig. 7) sampling range readings from transducer $S2$ would reveal the "right" edge of the obstacle.

There must always be two edges to add an entry to the temporary map. Before supplying new edge coordinates to the map, the coordinates are altered to artificially enlarge the obstacle boundary. The structure of the map, as well as the optimal path-finding algorithm mentioned later, are extensively described in a recent paper [3]. Note that this algorithm finds an optimal path (in terms of distance) through a room with known obstacles. Clearly, if the robot encounters an unexpected obstacle, optimality can no longer be guaranteed. However, consecutive application of the path-planning algorithm will take into account the added obstacle boundaries.

IV. Obstacle Avoidance Based on Inaccurate Sensory Information

The obstacle avoidance algorithm is best described with the aid of an example. One less successful experiment was chosen to visualize as many of the self-correcting features which constitute the basic idea of this algorithm as possible.

Fig. 8 shows the stationary map of our laboratory (as opposed to the temporary map which will be added later as unexpected obstacles are detected [19]). An XY-coordinate system is attached to two of the walls. In this example, the walls and one fixed obstacle (a laboratory table) are known to the robot system in advance (solid lines in Fig. 8). In the computer representation the obstacle boundaries are expanded by shifting them parallel to the real boundaries by a distance equal to half the width of the robot plus 10 cm as a safety factor. This representation is called the configuration space approach [6], [10], [18], [25] and allows the robot to be considered shrunken to a point which may move on the expanded boundaries. Corner points are numbered in Fig. 8 and serve as via points for optimal path calculations. Also in Fig. 8, the robot is shown as viewed from the top, with its flat side pointing forward.

Fig. 9 shows the "history" of the experiment. The robot is instructed to move from point O to F, but a chair was placed in its way, as shown in Fig. 9. Upon receiving the command, the robot turns on the spot (about its center point), until it faces into the direction of F. Then the robot moves on a straight line toward F. At this time the robot is unaware of the obstacle (the chair, which is plotted in its actual size as the rectangle $abcd$ in Fig. 9). At point A the ultrasonic sensor detects the presence of the obstacle, and the robot stops. The measuring mode is activated and yields the extended boundary line 9–10. Subsequently, the path-finding routine [3] is called, which suggests to detour the obstacle through 10 to F. The robot moves to 10, turns there until it faces F, and starts moving towards F. Immediately, the ultrasonic sensors issue another "obstacle alarm" and the robot stops at B. Again the obstacle is scanned, this time from a more favorable angle, and the robot comes up with an additional (extended) boundary: line 11–12. This time the path-finding routine suggests to pass through 12 to F. Following this route, the robot successfully reaches its destination.

What had happened is easily explained. On their first scan of the obstacle, from point A, the sensors received an echo only from corner a of the obstacle, whereas sides ad and ab, due to their unfavorable angle relative to the sensors, did not produce a detectable reflection. Thus both edges were (incorrectly) found to be close to a. Therefore, points 9 and 10, which represent the edges after

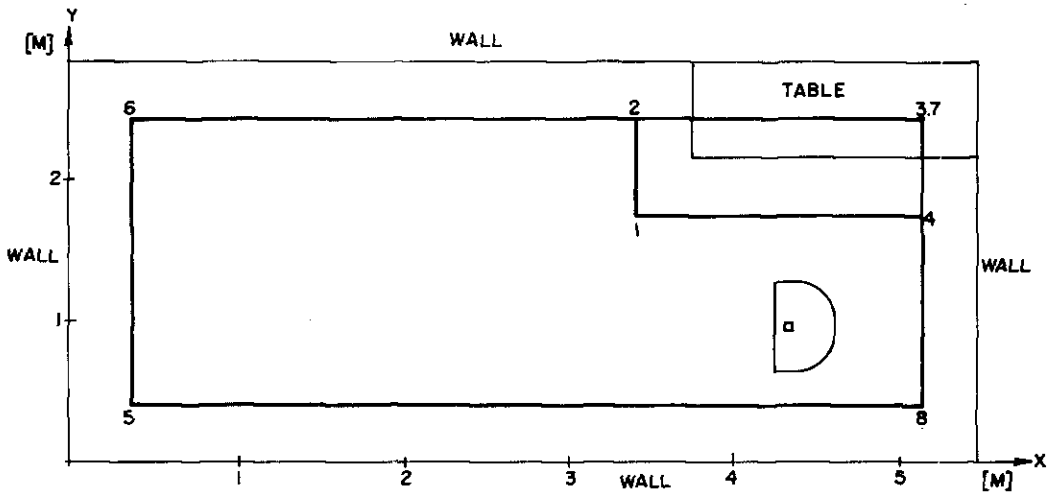

Fig. 8. Map of stationary obstacles.

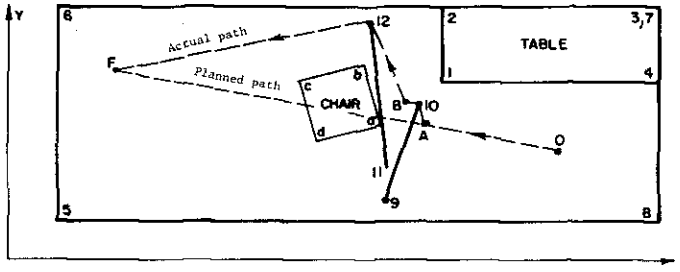

Fig. 9. Experimental test with unexpected obstacle.

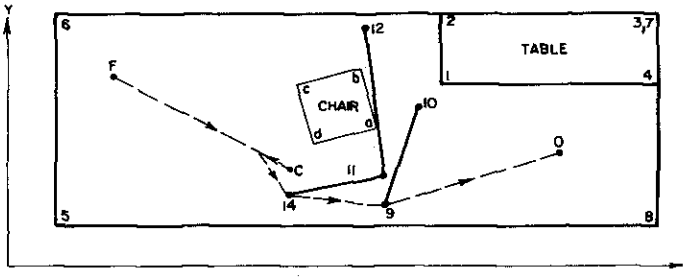

Fig. 10. Collision recovery in experimental test.

expansion, are too close to the real boundaries of the obstacle to allow the robot to successfully detour it. On the other hand, when viewing the obstacle from B, side ab produced a good reflection, and the actual edges a and b were found more accurately (and extended to points 11 and 12).

After the robot reached its destination, it was instructed to return back to its former starting point. The history of this journey is illustrated in Fig. 10. Since boundaries 9–10 and 11–12 are now known to the robot computer, the path-planning algorithm takes them into consideration and determines the shortest path to O to pass through 9. The robot starts its motion by turning on the spot at F until it faces point 9, and then starts moving straight forward toward 9. However, the outward pointing legs of the chair are not detected by the ultrasonic sensor, and the robot hits the obstacle with the leftmost part of its bumper. Notified by the microswitch attached to the bumper, the robot stops within a short distance which is smaller than the distance between bumper and robot body. This, together with the energy-absorbing design of the bumpers, keeps the wheel slippage insignificantly low (thus retaining validity of internal position information), even when the obstacle was hit at maximum speed. Subsequently, the robot performs a simple but effective collision recovery routine: moving 30 cm backwards, turning 30° to the right, and moving 50 cm forward. This routine has been found experimentally to be the most effective. Upon completing these motions, the robot reaches point 14, well outside of the danger zone. Standing at 14, the path planning algorithm suggests to pass through 9 to O, and the robot indeed reaches its destination uninterruptedly.

Hitting an obstacle with the bumper clearly shows that the obstacle has been mapped inaccurately. Learning from experience, a new boundary line, accounting for this incidence, should be added to the map. The new boundary line is defined by point 14 and the edge closest to this position, point 11.

In an additional run the robot was ordered to move to point F again. Based on its previously acquired knowledge of the obstacle, the path-planning routine suggests 9–14–F as the shortest possible path, and the robot reaches F without any interruptions.

Though the previous example is considered as a less successful run, there were even worse trials, especially when several "hard-to-detect" kind of obstacles were scattered around in such a way that the free gap between them was about the size of the robot width. In these cases the collision recovery algorithm showed a tendency to let the robot oscillate between the obstacles, adding more and more (almost identical) boundaries to the map. Since the number of boundaries in the map advertently influences the calculation time of the path-planning algorithm, it would take the robot several minutes to work its way around the obstacles. To avoid such situations, another algorithm has been incorporated in the program. If the robot found itself cut off from the destination by too many boundaries, the algorithm would simply wipe out the temporary map and the robot would try all over again. It should be stressed, however, that these are rare cases, caused by artificially produced extreme difficulties aimed at testing the recursively functioning recovery routines. Recursion in this case lends the robot a somewhat stubborn behavior which leads it, at times after considerable struggle, to its goal.

V. Conclusion

This paper discusses the obstacle avoidance algorithm used for a mobile robot. Since the algorithm depends heavily on the performance of the ultrasonic range finders, these sensors and the effect of their limitations on the obstacle avoidance algorithm were discussed as well.

REFERENCES

[1] G. Bauzil, M. Briot, and P. Ribes, "A navigation sub-system using ultrasonic sensors for the mobile robot HILARE," in *Proc. Ist Int. Conf. Robot Vision and Sensory Controls,* Apr. 1981, Stratford-upon-Avon, UK, pp. 47–58 and pp. 681–698.

[2] J. Borenstein and Y. Koren, "A mobile platform for nursing robots," *IEEE Trans. Ind. Electron.,* vol. IE-32, pp. 158–165, May 1985.

[3] ——, "Optimal path algorithms for autonomous vehicles," in *Proc. 18th CIRP Manufacturing Systems Seminar,* June 1986, Stuttgart, Germany.

[4] ——, "Motion control analysis of a mobile robot," *Trans. ASME, J. Dynamics, Meas., Contr.,* vol. 109, no. 2, pp. 73–79, June 1987.

[5] J. A. Boyle, "Robotic steering," Internal Project of the Trent Polytechnic, Nottingham, England, 1982.

[6] R. A. Brooks, "Solving the find-path problem by good representation of free space," in *Proc. Nat. Conf. Artificial Intelligence, AAAI-82,* Aug. 1982, pp. 381–386.

[7] S. Ciarcia, "Home in the range, An ultrasonic ranging system," *BYTE,* Nov. 1980.

[8] R. A. Cooke, "Microcomputer control of free ranging robots," in *Proc. 13th Int. Symp. Industrial Robots and Robots,* Chicago, IL, Apr. 1983, pp. 13.109–13.120.

[9] J. L. Crowley, "Dynamic world modeling for an intelligent mobile robot," in *IEEE 7th Int. Conf. Pattern Recognition Proc.,* 1984, Montreal, PQ, Canada, pp. 207–210.

[10] ——, "Navigation for an intelligent mobile robot," *Carnegie-Mellon* University, The Robotics Institute, Pittsburgh, PA, Tech. Rep., Aug. 1984.

[11] H. R. Everett, "A second-generation autonomous sentry robot," *Robotics Age,* pp. 29–32, Apr. 1985.

[12] ——, "A multielement ultrasonic ranging array," *Robotics Age,* pp. 13–20, July 1985.

[13] C. Helmers, "Ein heldenleben," *Robotics Age,* pp. 7–16 and pp. 44–45, Mar./Apr. 1983.

[14] J. P. Hermann *et al.,* "Pattern recognition in the factory: An example," in *Proc. 12th Int. Symp. Industrial Robots,* Paris, France, 1982, pp. 271–280.

[15] G. Hoffstatter, "Using the Polaroid ultrasonic ranging system," *Robotics Age,* pp. 35–37, Sept. 1984.

[16] J. Iijima, S. Yuta, and Y. Kanayama, "Elementary functions of a self-contained robot 'YAMABICO 3.1'," in *Proc. 11th Int. Symp. Industrial Robots,* Tokyo, Japan, 1983, pp. 211–218.

[17] D. L. Jaffe, "Polaroid ultrasonic ranging sensors in robotic applications," *Robotic Age,* pp. 23–30, Mar. 1985.

[18] C. Jorgensen, W. Hamel, and C. Weisbin, "Autonomous robot navigation," *BYTE,* pp. 223–235, Jan. 1986.

[19] D. M. Keirsey *et al.,* "Algorithm of navigation for a mobile robot," in *Proc. Ist Int. Conf. Robotics,* Atlanta, GA, Mar. 1984, pp. 574–583.

[20] H. Kuttruff, *Room Acoustics,* 2nd ed. London: Applied Science Publishers, 1979, pp. 77–80.

[21] D. Lampe, "Robot sentries," *Popular Sci.,* p. 20, Aug. 1985.

[22] L. Leifer, "Rehabilitative robotics, The Stanford robotic aid," presented at the Robotics West Conf., Sept. 1981.

[23] ——, "Rehabilitative robots," *Robotics Age,* pp. 4–14, May 1981.

[24] P. W. K. Lau, Robotic steering, "Internal Project of the Trent Polytechnic, Nottingham, England, 1981.

[25] T. Lozano-Perez, "Automatic planning of manipulator transfer movements," *IEEE Trans. Syst., Man., Cybern.,* vol. SMC-11, pp. 681–698, Oct. 1981.

[26] G. D. Maslin, "A simple ultrasonic ranging system," presented at the 102nd Convention of the Audio Engineering Society, Cincinnati, OH, May 12, 1983 (reprinted in *POLAROID Ultrasonic Ranging System Handbook, Application Notes/Technical Papers,* supplied with sensor hardware kit).

[27] H. P. Moravec and A. Elfes, "High resolution maps from wide angle sonar," presented at the IEEE Conf. Robotics and Automation, 1985.

[28] P. M. Morse, *Vibration and Sound,* 2nd ed. New York: McGraw-Hill, 1948, pp. 326–329.

[29] H. F. Olson, *Acoustical Engineering,* 3rd ed. Princeton, NJ: Van Nostrand, 1957, pp. 20–23.

[30] *Ultrasonic Ranging System,* Polaroid Corporation, 1982.

[31] C. Quick, "Animate versus inanimate," *Robotics Age,* pp. 15–17, Aug. 1984.

The Analysis of Equilateral Grip of a Prismatic and Convex Workpiece

M. ORLOWSKI AND M. PACHTER

***Abstract*—Certain facets of the gripping problem in robotics are discussed. We consider a gripper with a single degree of freedom that consists of three equal-length fingers, and we model the set of workpieces under consideration by prismatic and convex polyhedra. We are thus led to a planar-geometric formulation, and then address the computational geometric problem of inscribing, in a given convex polygon, an equilateral triangle that is locally minimal. Feasibility and the (computational) geometric construction of the solution are emphasized.**

I. INTRODUCTION

In this correspondence, we address certain conceptual facets of the gripping problem in robotics. In most robots [1] the gripping end consists of two fingers. Thus if we confine our attention to prismatic and convex workpieces, we observe that the problem is reduced to a planar-geometric situation, as is illustrated in Fig. 1 for the special case of a smooth workpiece. In Fig. 2(a) and (b) we give a schematic illustration of the two gripping ends designed to hold the workpiece from the outside and the inside, respectively; in the latter case we imagine the convex figure shown in Fig. 1 to represent the boundary of a convex hole in the workpiece from which the workpiece can be engaged from the inside by the gripping mechansim shown in Fig. 2. Also, note that the gripping mechanism is spring-loaded, and in Fig. 2(a) the spring works in tension, whereas in Fig. 2(b) it works in compression.

In view of the above, it is evident that the solution to the two-finger gripping problem is provided by the drawing in Fig. 1. Namely, to hold the workpiece from the outside one must apply the two fingers of the gripper to the points A and B, that delimit the width of the convex workpiece, whereas to secure the workpiece from the inside one must apply the two fingers of the gripper shown in Fig. 2(b) to the points C and D that delimit the diameter of the convex hole in the workpiece. We do not here discuss the existence and the calculation of the above four points A, B, C, and D, and the interested reader is referred to [2]. It suffices to say that the stated solution to the gripping problem is stable—that is, a small perturbation of the fingers of the gripper shown in Fig. 2(a) away from the contact points A and B results in a restoring torque. Similarly, a small perturbation of the fingers of the gripper shown in Fig. 2(b) away from the contact points C and D also results in a restoring torque. In this respect, the drawings of Fig. 3(a) and (b) are self-explanatory. Furthermore, stability also follows from the alternative observation that $|AB| < |A'B'|$ and $|CD| > |C'D'|$, which in turn implies that the potential energy (stored in the spring) of the system is locally minimal in Fig. 3(a) and locally maximal in Fig. 3(b) which, according to the Lagrangian formulation, implies stability.

However, in the more general case where the workpiece is piecewise smooth, or in the case where the workpiece is modeled by a convex polygon to fit the usual paradigm of computational geometry, stability when gripping from the outside (with the gripper shown in Fig. 2(a)) is in general unattainable, except in the special case where the sides of the polygon adjacent to the vertices A and B in Fig. 1 are parallel. This is what motivates us to explore the possibilities of a single degree of freedom gripper that consists of three fingers of equal length, which we refer to as the equilateral grip situation. This concept is schematically illustrated in Fig. 4. Here, a single degree of

Manuscript received January 7, 1986; revised June 29, 1987.

The authors are with the National Research Institute for Mathematical Sciences of the CSIR, P.O. Box 395, Pretoria 0001, South Africa.

IEEE Log Number 8718082.

0882-4967/88/0400-0218$01.00 © 1988 IEEE